NASA Technical Memorandum 103236

Application of Mixing-Controlled Combustion Models to Gas Turbine Combustors

Hung Lee Nguyen
Lewis Research Center
Cleveland, Ohio

Prepared for the
Joint Symposium on General Aviation Systems
cosponsored by the AIAA and FAA
Ocean City, New Jersey, April 11–12, 1990

NASA

APPLICATION OF MIXING-CONTROLLED COMBUSTION MODELS TO GAS TURBINE COMBUSTORS

Hung Lee Nguyen
National Aeronautics and Space Administration
Lewis Research Center
Cleveland, Ohio 44135

Summary

This report describes the study of exhaust gas emissions from a staged Rich Burn/Quick-Quench Mix/Lean Burn (RQL) combustor under test conditions encountered in High Speed Research (HSR) engines. The combustor was modeled at conditions corresponding to different engine power settings, and the effect of primary dilution airflow split on emissions, flow field, flame size and shape, and combustion intensity, as well as mixing, was investigated. A mathematical model was developed from a two-equation model of turbulence, a quasi-global kinetics mechanism for the oxidation of propane, and the Zeldovich mechanism for nitric oxide formation. A mixing-controlled combustion model was used to account for turbulent mixing effects on the chemical reaction rate. This model assumes that the chemical reaction rate is much faster than the turbulent mixing rate. The work described in this report is a part of the NASA High Speed Research Low NO_x program.

Introduction

Future gas turbine engines are expected to operate at higher pressure ratios, inlet-air temperatures, and fuel-air ratios. At these conditions, conventional combustors would produce high levels of oxides of nitrogen (NO_x).Nitric oxides are divided into two classes according to their mechanism of formation: (1) "thermal NO_x," which is primarily nitric oxide (NO) with a small percentage of nitrogen dioxide (NO_2), is formed from the oxidation of diatomic nitrogen in the combustion air and fuel; and (2) "organic NO_x" is formed by oxidation of organically bound nitrogen in the fuel (fuel-bound nitrogen (FBN)). The main factors governing the thermal NO_x formation rate are flame temperature and residence time; therefore, these factors must be lowered in order to reduce NO_x formation. Organic NO_x formation is less well understood than thermal NO_x formation; however, we do know that measures which reduce flame temperature and thereby abate thermal NO_x have little effect, positive or even adverse, an organic NO_x. In this study, only thermal NO_x is considered.

Two promising concepts for reducing NO_x emissions of advanced engines are the lean, premixed prevaporized (LPP) and the Rich Burn/Quick-Quench Mix/Lean Burn (RQL) combustors. The RQL concept (refs. 1 to 5) incorporates staged burning. Combustion is initiated in a fuel-rich zone with an equivalence ratio in the range of 1.2 to 1.8. The hydrocarbon reactions proceed rapidly, thereby depleting the available oxygen and inhibiting NO_x formation. Additional air is then added, and combustion is completed under excess-air conditions. Combustion takes place in the rich and lean zones at temperatures well below the stoichiometric flame temperature, so NO_x production is minimized.

The lean, premixed prevaporized (LPP) combustor is another method of flame-temperature control, in addition to using variable geometry features to control the stoichiometry of the primary combustion zone (refs. 6 to 8). In this approach, increasing the amount of primary zone air decreases NO_x emissions by reducing both flame temperature and residence time.

In this study we consider a two-dimensional, confined swirling flow, staged RQL combustor model and study the combustor characteristics for a range of operating conditions. In the following sections the problem is formulated, the combustion models and numerical procedure are described, and the results are presented.

Model Description

The combustor consists of a primary and a secondary zone. The fuel (propane) and primary air are fed to the combustor via two confined, coaxial, swirling jets, with propane in the inner jet and air in the outer jet. Additional quick-quench air is fed to the secondary zone through the holes located on the

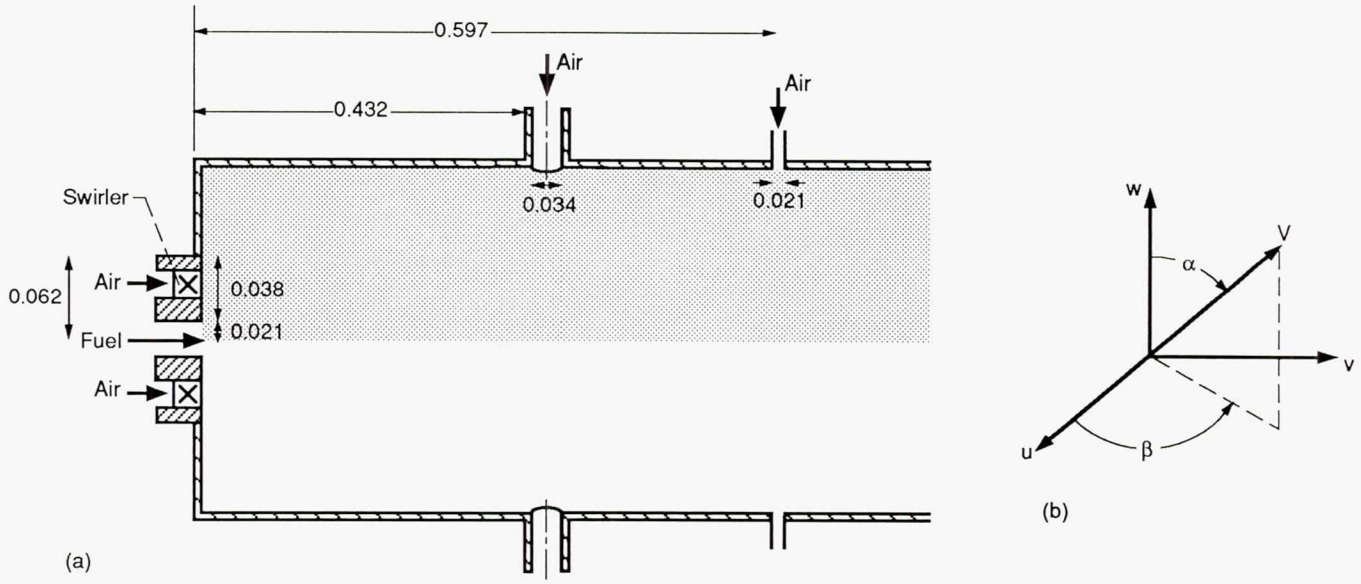

(a) Schematic of combustor model (dimensions are in meters).
(b) Dilution jets velocity prolfile.

Figure 1—Staged combustor and possible orientation of secondary swirling air jets.

combustor liner. A schematic of the staged combustor, together with possible orientation of the secondary swirling air jets, is shown in figure 1.

Governing Equations

The governing equations for a turbulent axisymmetric, compressible, steady, and swirling flow case are considered. The general equations representing the conservation of mass and momentum for two-dimensional steady flows can be written in cylindrical coordinates (ref. 9) as continuity,

$$\frac{1}{r}\frac{\partial}{\partial r}(r\rho v) + \frac{\partial}{\partial z}(\rho\mu) = 0 \tag{1}$$

the axial (u) momentum component,

$$\frac{1}{r}\frac{\partial}{\partial r}\left[r\left(\rho uv - \mu_{\text{eff}}\frac{\partial u}{\partial r}\right)\right] + \frac{\partial}{\partial z}\left(\rho uu - \mu_{\text{eff}}\frac{\partial u}{\partial z}\right) = -\frac{\partial p}{\partial z} + \frac{1}{r}\frac{\partial}{\partial r}\left(r\mu_{\text{eff}}\frac{\partial v}{\partial z}\right) + \frac{\partial}{\partial z}\left(\mu_{\text{eff}}\frac{\partial u}{\partial z} - \frac{2}{3}\rho k - \frac{2}{3}\mu_{\text{eff}}\,\nabla\cdot\vec{v}\right) \tag{2}$$

the radial (v) momentum component,

$$\frac{1}{r}\frac{\partial}{\partial r}\left[r\left(\rho vv - \mu_{\text{eff}}\frac{\partial v}{\partial r}\right)\right] + \frac{\partial}{\partial z}\left(\rho uv - \mu_{\text{eff}}\frac{\partial v}{\partial z}\right) = -\frac{\partial p}{\partial r} + \rho\frac{w^2}{r} + \frac{1}{r}\frac{\partial}{\partial r}\left[r\left(\mu_{\text{eff}}\frac{\partial v}{\partial r} - \frac{2}{3}\rho k - \frac{2}{3}\mu_{\text{eff}}\,\nabla\cdot\vec{v}\right)\right] + \frac{\partial}{\partial z}\left(\mu_{\text{eff}}\frac{\partial u}{\partial r}\right) - 2\mu_{\text{eff}}\frac{v}{r^2} + \frac{2}{3}\frac{\rho k}{r} + \frac{2}{3}\frac{\mu_{\text{eff}}}{r}\,\nabla\cdot\vec{v} \tag{3}$$

and the azimuthal (w) momentum component,

$$\frac{1}{r}\frac{\partial}{\partial r}\left[r\left(\rho vw - \mu_{\text{eff}}\frac{\partial w}{\partial r}\right)\right] + \frac{\partial}{\partial z}\left(\rho uw - \mu_{\text{eff}}\frac{\partial w}{\partial z}\right) + \rho\frac{vw}{r} = -\frac{w}{r^2}\frac{\partial}{\partial r}(r\mu_{\text{eff}}) \tag{4}$$

where the following modeling of fluctuating quantities has been used:

$$-\rho\overline{u'v'} = \mu_t\left(\frac{\partial u}{\partial r} + \frac{\partial v}{\partial z}\right) \tag{5}$$

$$-\rho\overline{u'u'} = 2\mu_t\frac{\partial u}{\partial z} - \frac{2}{3}\rho k - \frac{2}{3}\mu_t\,\nabla\cdot\vec{v} \tag{6}$$

$$-\rho\overline{v'v'} = 2\mu_t \frac{\partial v}{\partial r} - \frac{2}{3}\rho k - \frac{2}{3}\mu_t \nabla \cdot \vec{v} \tag{7}$$

$$-\rho\overline{w'w'} = 2\mu_t \frac{v}{r} - \frac{2}{3}\rho k - \frac{2}{3}\mu_t \nabla \cdot \vec{v} \tag{8}$$

$$-\rho\overline{u'w'} = -\rho\overline{v'w'} = 0 \tag{9}$$

$$\mu_{\text{eff}} = \mu_t + \mu \tag{10}$$

$$\mu_t = C_\mu \rho k^{1/2} \ell \tag{11}$$

$$\nabla \cdot \vec{v} = \frac{1}{2}\frac{\partial}{\partial r}(vr) + \frac{\partial u}{\partial z} \tag{12}$$

Turbulence Modeling

The effect of turbulence is included by means of a k-ε model. The differential equation for turbulence kinetic energy k is

$$\frac{1}{r}\frac{\partial}{\partial r}\left[r\left(\rho vk - \mu_{\text{eff}}\frac{\partial k}{\partial r}\right)\right] + \frac{\partial}{\partial z}\left(\rho uk - \mu_{\text{eff}}\frac{\partial k}{\partial z}\right) = P - \rho\varepsilon \tag{13}$$

where

$$P = \mu_{\text{eff}}\left[2\left(\frac{\partial u}{\partial z}\right)^2 + 2\left(\frac{\partial v}{\partial r}\right)^2 + 2\left(\frac{v}{r}\right)^2 + \left(\frac{\partial w}{\partial r} - \frac{w}{r}\right)^2 + \left(\frac{\partial u}{\partial r} + \frac{\partial v}{\partial z}\right)^2 + \left(\frac{\partial w}{\partial z}\right)^2\right] \tag{14}$$

and that for the dissipation rate of turbulence kinetic energy ε is

$$\frac{1}{r}\frac{\partial}{\partial r}\left[r\left(\rho v\varepsilon - \frac{\mu_{\text{eff}}}{\sigma_\varepsilon}\frac{\partial \varepsilon}{\partial r}\right)\right] + \frac{\partial}{\partial z}\left(\rho u\varepsilon - \frac{\mu_{\text{eff}}}{\sigma_\varepsilon}\frac{\partial \varepsilon}{\partial z}\right) = C_1\frac{\varepsilon}{k}p - C_2\rho\frac{\varepsilon^2}{k} \tag{15}$$

In the foregoing equations, r and z are the radial and axial coordinates measured from the combustor centerline and combustor inlet, respectively; ρ is the mean flow density; u, v, and w are the mean flow axial, radial, and azimuthal velocity components, respectively; p is the pressure; P is the production rate of turbulence kinetic energy; and the effective viscosity μ_{eff} is the sum of the laminar (μ) and turbulence (μ_t) viscosities. A scalar (isotropic) turbulence viscosity is assumed; C_μ, C_1, C_2, and σ_ε are turbulence model constants, and the primes denote fluctuating quantities. The values of the turbulence constants are given in table I.

Thermal and Reacting Flows

The stagnation enthalpy equation can be written as

$$\frac{1}{r}\frac{\partial}{\partial r}\left[r\left(\rho vH - \mu_{\text{eff}}\frac{\partial H}{\partial r}\right)\right] + \frac{\partial}{\partial z}\left(\rho uH - \mu_{\text{eff}}\frac{\partial H}{\partial z}\right) = 0 \tag{16}$$

where the laminar and turbulence Prandtl numbers have been assumed equal to one, and the mean flow stagnation enthalpy H is defined as

$$H = \frac{1}{2}(u^2 + v^2 + w^2) + \sum_{j=1}^{5} Y_j h_j^0 + \sum_{j=1}^{5} Y_j \int_{T_0}^{T} C_p\, dT \tag{17}$$

where Y_j is the concentration of species j; h_j^0 is the enthalpy of formation of species j at the reference temperature $T_0 = 298.15$ K; C_p is the specific heat at constant pressure; T is the temperature; and the five chemical species considered are C_3H_8, O_2, N_2, CO_2, and H_2O.

The combustion of propane is modeled by using the one-step global mechanism:

$$C_3H_8 + 5(O_2 + 3.76N_2) \rightarrow 3CO_2 + 4H_2 + 18.8N_2 \tag{18}$$

The oxidation of fuel is controlled by the chemical reaction rate. This reaction rate is controlled either by the mixing of eddies (mixing-controlled) that contain reactants and products or by an Arrhenius rate equation (chemical kinetics controlled). In this investigation, the mixing-controlled model is used. In the mixing-controlled model, the influence of turbulence on the reaction rate is taken into account by assuming that the generation and the dissipation of the time-average of the square of the fuel concentration fluctuations are equal:

$$Cg_1\rho k^{1/2}\varepsilon\left[\left(\frac{\partial Y_f}{\partial r}\right)^2 + \left(\frac{\partial Y_f}{\partial z}\right)^2\right] = Cg_2\rho\frac{k^{1/2}}{\varepsilon}y_f^2 \tag{19}$$

where Y_f is the mean fuel (propane) mass fraction, y_f is the fluctuating mass fraction of fuel, and Cg_1 and Cg_2 are constants.

The mean reaction rate of the fuel R_f can be written as

$$R_f = Cg_3\rho\sqrt{y_f^2}\frac{k^{1/2}}{\varepsilon} = C\rho k^{1/2}\sqrt{\left(\frac{\partial Y_f}{\partial f}\right)^2 + \left(\frac{\partial Y}{\partial x}\right)^2} \tag{20}$$

TABLE I.—VALUES OF MODEL CONSTANTS

Turbulence model			Mixing-controlled model			
C_μ	C_1	C_2	Cg_1	Cg_2	Cg_3	C
0.09	1.44	1.0	2.70	0.134	0.00456	0.02

where

$$C = Cg_3\sqrt{\frac{Cg_1}{Cg_3}}$$

The values of the mixing-controlled reaction rate model constants are shown in table I.

Species Equation

If the laminar and turbulence Schmidt numbers for all species are assumed equal to one, the following equations are obtained for the time-averaged mass fractions:

$$\frac{1}{r}\frac{\partial}{\partial r}\left[r\left(\rho v Y_f - \mu_{eff}\frac{\partial Y_f}{\partial r}\right)\right] + \frac{\partial}{\partial z}\left(\rho u Y_f - \mu_{eff}\frac{\partial Y_f}{\partial z}\right) = -R_f \tag{21}$$

$$\frac{1}{r}\frac{\partial}{\partial r}\left[r\left(\rho v Y_n - \mu_{eff}\frac{\partial Y_n}{\partial r}\right)\right] + \frac{\partial}{\partial z}\left(\rho u Y_n - \mu_{eff}\frac{\partial Y_n}{\partial z}\right) = 0 \tag{22}$$

$$\frac{1}{r}\frac{\partial}{\partial r}\left[r\left(\rho v Y_{sz} - \mu_{eff}\frac{\partial Y_{sz}}{\partial r}\right)\right] + \frac{\partial}{\partial z}\left(\rho u Y_{sz} - \mu_{eff}\frac{\partial Y_{sz}}{\partial z}\right) = 0 \tag{23}$$

where

$$Y_{sz} = sY_f - Y_0 \tag{24}$$

$$Y_p = 1 - Y_f - Y_0 - Y_n \tag{25}$$

s is the reaction stoichiometric coefficient; Y_0, Y_n, and Y_p are the mass fractions of the oxidizer, nitrogen, and combustion products, respectively; and Y_{sz} is the mass fraction of the Shvab-Zeldovich variable used in the Zeldovich mechanism for nitric oxide formation.

Equation of State

The density can be calculated from the equation of state:

$$\rho = \frac{P}{RT}\sum_{j=1}^{5}\left(\frac{Y_j}{W_j}\right) \tag{26}$$

where R is the universal gas constant and W denotes molecular weight.

Boundary Conditions

At the combustor inlet the flow was assumed to have a zero mean radial velocity, and uniform axial velocity and pressure. The azimuthal velocity profile of the inner (fuel) jet was simulated by a solid body rotation, whereas that of the outer (inlet-air) jet was modeled by a free vortex. The temperatures of the fuel and inlet-air jets were assumed to be uniform and equal to 300 and 1000 °F, respectively. The inlet profiles of turbulence kinetic energy taken from references 10 and 11 are as follows:

$$k(r,0) = \begin{cases} (0.035u_i)^2\left[2+8\left(\dfrac{r}{R_i}\right)^2\right] & 0 \le r \le R_i \\ (0.035u_o)^2\left[2+4\left(\dfrac{r}{R_s}\right)^2+4\left(\dfrac{r}{R_o}\right)^2\right] & R_s \le r \le R_o \end{cases} \tag{27}$$

$$\varepsilon(r,0) = \begin{cases} k^{3/2}(r,0)/0.005R_i \\ k^{3/2}(r,0)/0.005R_o \end{cases} \tag{28}$$

where R_i and R_o are the inner radii of the fuel and inlet-air pipes, respectively; R_s is the outer radius of the fuel pipe; and u_i and u_o are the mean axial velocities of the fuel and inlet-air jets, respectively. The combustor geometry and dimensions are shown in figure 1(a).

At the combustor centerline (symmetry axis) both the radial and azimuthal velocity components are zero, whereas the radial derivatives of the other flow quantities are zero. At the combustor outlet, the flow is assumed to leave with zero axial derivatives. At solid walls the normal velocity component to the walls was set to zero, and the law-of-the-wall was used to calculate the tangential velocity near the walls. The solid-wall temperature was assumed equal to 350 K. The Reynolds analogy was used to calculate the heat transfer loss through the solid walls.

The boundary conditions of the quick-quench mixing jet and the dilution jets can be summarized as follows:

$$u_j = V \sin\alpha \cos\beta$$

$$v_j = V \sin\alpha \sin\beta$$

$$w_j = V \cos\alpha$$

where u_j, v_j, and w_j are the velocity components of the jets and V, α, and β are shown in figure 1(b). Both of the jets'

mass flow rates and pressures are prescribed. The inlet profiles of the jets' turbulence kinetic energy are similar to that of the combustor's inlet fuel jet.

Numerical Method

The numerical procedure employed in the calculations herein is of the control volume variety (ref. 12). It uses a staggered grid and an implicit finite-difference algorithm. Calculations were made by a hybrid numerical technique that uses control differences for the convection terms whenever the absolute value of the mesh Reynolds number is smaller than two, and uses upwind differences when the absolute value is greater than two. The calculations were performed in the following manner. First, a value for an initial pressure field was assumed and employed to calculate the corresponding velocity field. Then a Poisson equation for the pressure field was formulated and taken to be equal to the sum of the assumed field value plus a local pressure perturbation. The solution of the Poisson equation yields the new pressure, which is generally different from the guessed one. Therefore, the momentum and Poisson equations were solved iteratively until a prescribed convergence criterion (error tolerance) was satisfied. A grid consisting of 32 by 32 points was used in the calculations.

Results and Discussion

Calculated results are presented here for the Rich Burn/Quick-Quench Mix/Lean burn combustor. The 13 different flow conditions that were studied are listed in table II. In figures 2 to 8 the profiles of the velocity vectors, stream function density, turbulence intensity ($i = \sqrt{2k/3}/u_i$), gas temperature, NO_x distribution, and fuel, oxygen, nitrogen, carbon dioxide, and water distributions for Φ_{RZ} (rich-zone equivalence ratio) = 1.65 (case 8) are presented. Figure 2 presents the mean velocity vectors showing magnitude and direction for a counter-swirl condition, that is, the fuel and inlet-air jets are counter-swirling. The inlet flow is lifted by centrifugal forces and creates a recirculation zone at the combustor centerline. The recirculation zone is characterized by a steep axial and azimuthal velocity gradient. A negative velocity, which appears at the location where the recirculation zone starts rolling up, disappears as the recirculation zone approaches the combustor inlet. The inlet-air flow shows a more uniform axial velocity profile along the recirculation zone and has a very steep velocity gradient at the shear layer regions of the incoming jets. The radial distribution of the velocity flattens out and becomes uniform as the velocity differs radially and axially downstream of the recirculation zone along the combustor. Figure 2 also shows that the quick-quench mixing

TABLE II.—RQL COMBUSTOR OPERATING CONDITIONS
[Inlet temperature, 1000 K; inlet pressure, 2.0 atm.]

Case number	Rich-zone equivalence ratio, ϕ_{RZ}	Quick-quench zone equivalence ratio	Lean-zone equivalence ratio
1	1.09	0.81	0.79
2	1.19	.83	.81
3	1.21	.78	.76
4	1.28	.84	.82
5	1.40	.95	.93
6	1.43	.78	.76
7	1.50	.72	.70
8	1.65	.79	.77
9	1.80	.86	.84
10	2.09	.89	.87
11	1.50	.77	.75
12	1.50	.80	.78
13	1.50	.82	.80

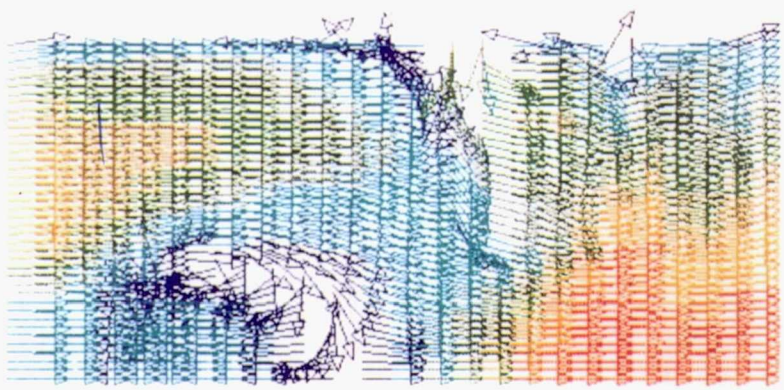

Figure 2.—Mean velocity vector profile for a rich-zone equivalence ratio of 1.65.

jet penetrates radially into two-thirds of the combustor radius, and that a portion of the quick-quench mixing jet recirculates upstream and creates a pair of lopsided vorticies sandwiching the jet. The dilution jet penetration is much less pronounced since the dilution jet-to-mainstream momentum flux ratio is lower than the quick-quench jet-to-mainstream momentum flux ratio. Comparison with the stream function density profile shown in figure 3 confirms the flow structure and dynamics observed from the velocity profile.

Figure 4 presents the turbulence intensity profile along the combustor. The turbulence intensity at the shear layer regions is much smaller than that in the recirculation zone. The high turbulence intensity observed in the recirculation zone and the lean-zone region downstream of the quick-quench mixing jet can be attributed to the high turbulence viscosity in these regions. The large radial gradient of the azimuthal velocity component in the recirculation zone results in a high production and dissipation rate of turbulence kinetic energy in this region. The high diffusion of axial and azimuthal velocity components in the lean-zone region downstream of the quick-quench mixing jet accounts for the large generation and dissipation rates of turbulence kinetic energy in this region. Turbulence is generated in regions of steep velocity gradients, for example, at the shear layer regions, since the turbulence kinetic energy produced is proportional to the square of the velocity gradients.

Figure 5 shows the mean temperature profile of the gas along the combustor. Note that the temperature is high in regions with high turbulence intensity. This is due to better mixing

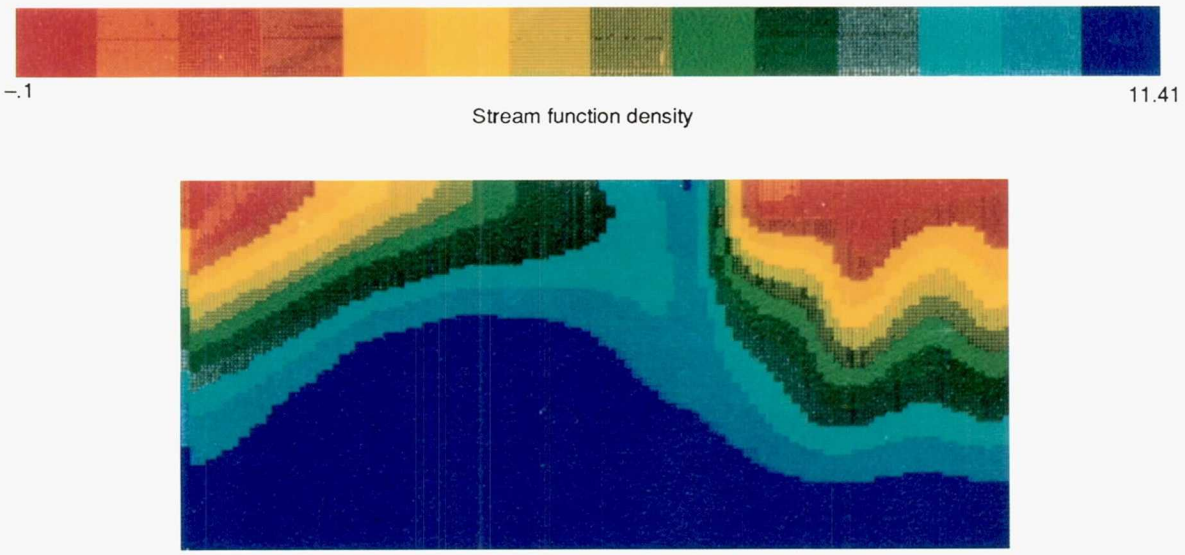

Figure 3.—Stream function density profile for a rich-zone equivalence ratio of 1.65.

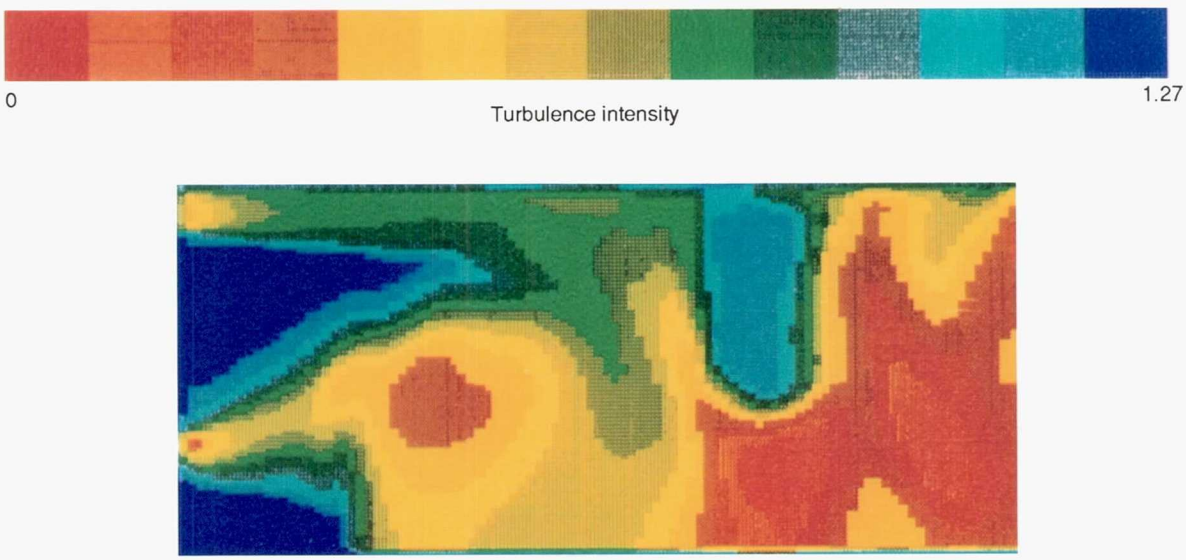

Figure 4.—Turbulence intensity profile for a rich-zone equivalence ratio of 1.65.

and the higher reaction rate that occurs in these regions. Most of the reactions take place at the rear of the high-pressure core of the recirculation zone and in the fuel-lean region downstream of the quick-quench mixing jet. Quenching takes place in the quick-quench mixer region because of the high-flow rate, quick-quench mixing air injected through the single hole on the two-dimensional combustor wall. An overall equivalence ratio of 0.5 is thus achieved. This results in very low combustion efficiency in this region.

The NO_x distribution along the combustor is shown in figure 6; it is highest in the lean-zone region, which would be expected since NO_x formation is proportional to flame temperature, residence time, and the availability of oxygen. The formation rate of NO_x is much smaller than the oxidation rates of hydrocarbon fuel and CO.

Figure 7 shows fuel vapor, oxygen, and nitrogen distribution. The fuel-rich region located at the front end of the recirculation zone accounts for a temperature that is lower in this region than at the rear end of the recirculation zone. Comparison of the fuel, oxygen, and nitrogen distributions confirms the observations made from the temperature and NO_x profiles. Figure 8 presents the carbon dioxide and water distributions along the combustor. The distribution of these combustion products agrees with the predicted flame temperature and fuel and oxygen profiles.

In figure 9 we summarize the data on NO_x concentration as a function of the rich-zone equivalence ratio. These data indicate that as the rich-zone equivalence ratio increases from 1.19 to 2.0, the NO_x concentration decreases.

Figure 10 shows the radial profile of combustor exit temperatures for cases 11 to 13. The maximum temperature is highest for case 13. The combustor liner heat transfer profiles are shown in figure 11 for cases 11 to 13.

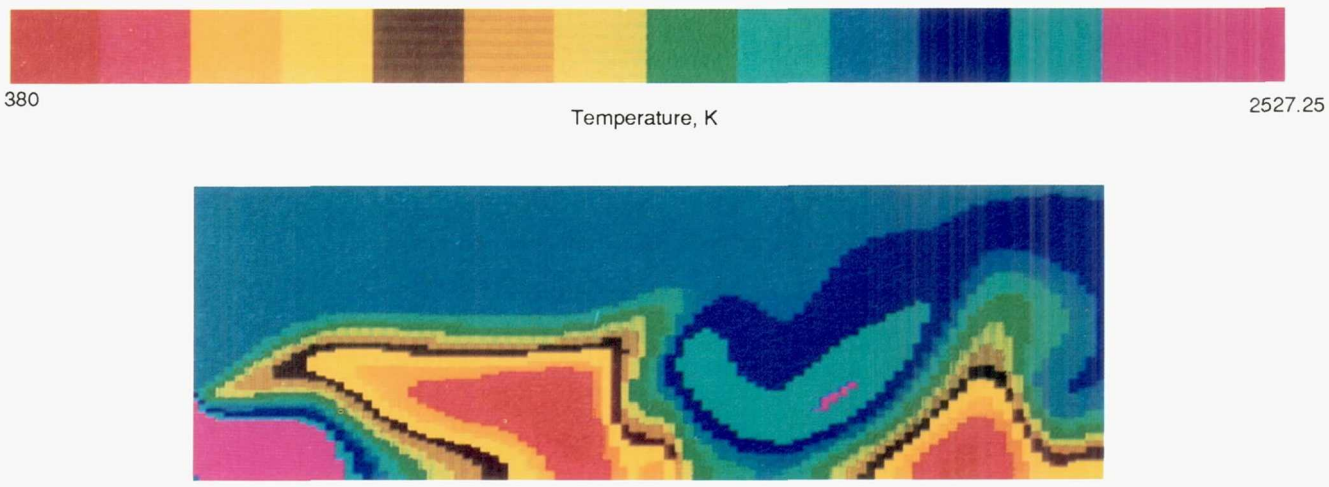

Figure 5.—Temperature distribution for a rich-zone equivalence ratio of 1.40.

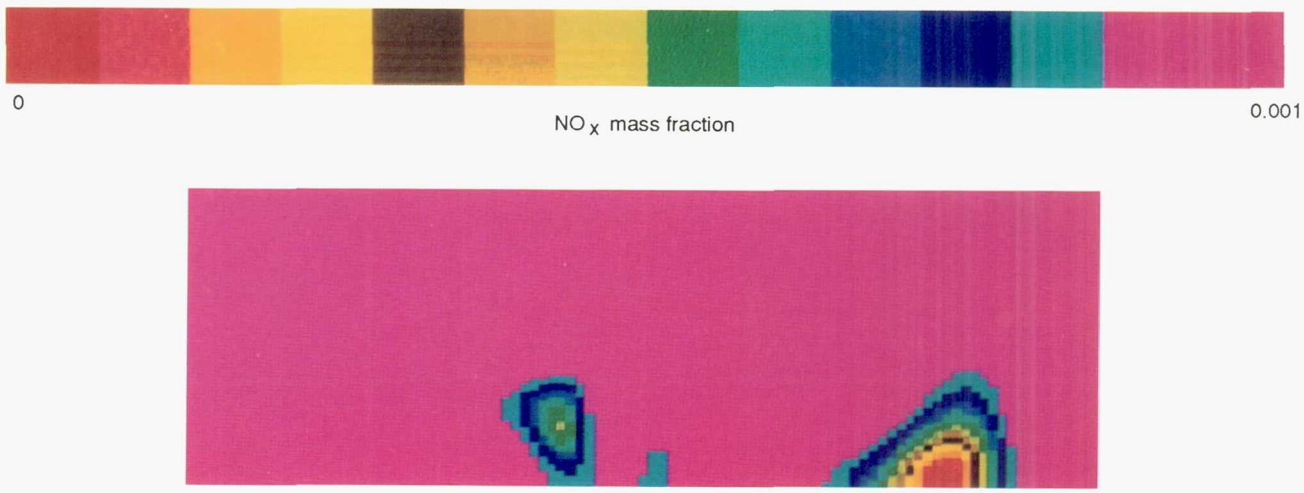

Figure 6.—NO_x mass fraction distribution for a rich-zone equivalence ratio of 1.40.

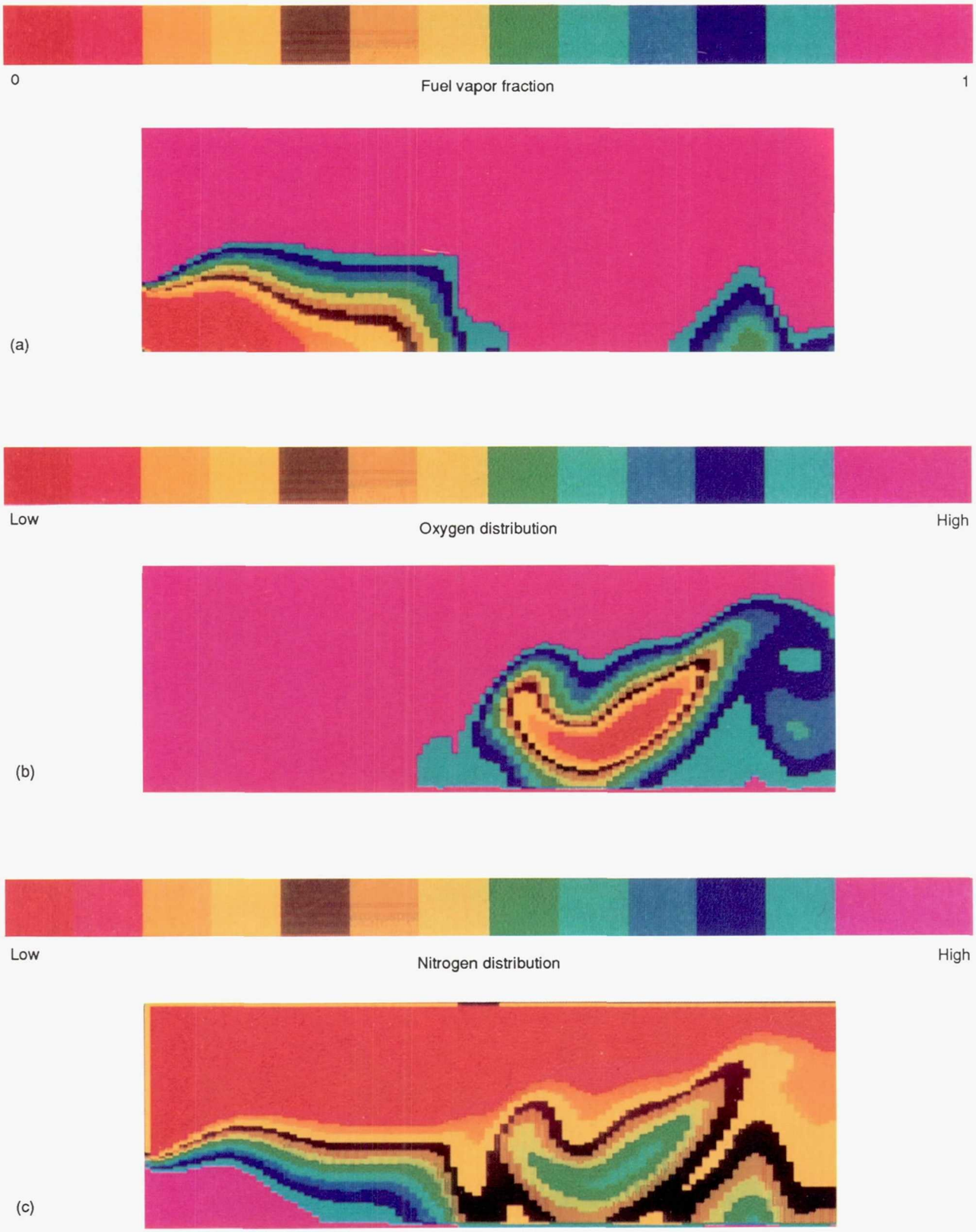

(a) Fuel vapor distribution.
(b) Oxygen distribution.
(c) Nitrogen distribution.

Figure 7.—Fuel vapor, oxygen, and nitrogen distributions for a rich-zone equivalence ratio of 1.40.

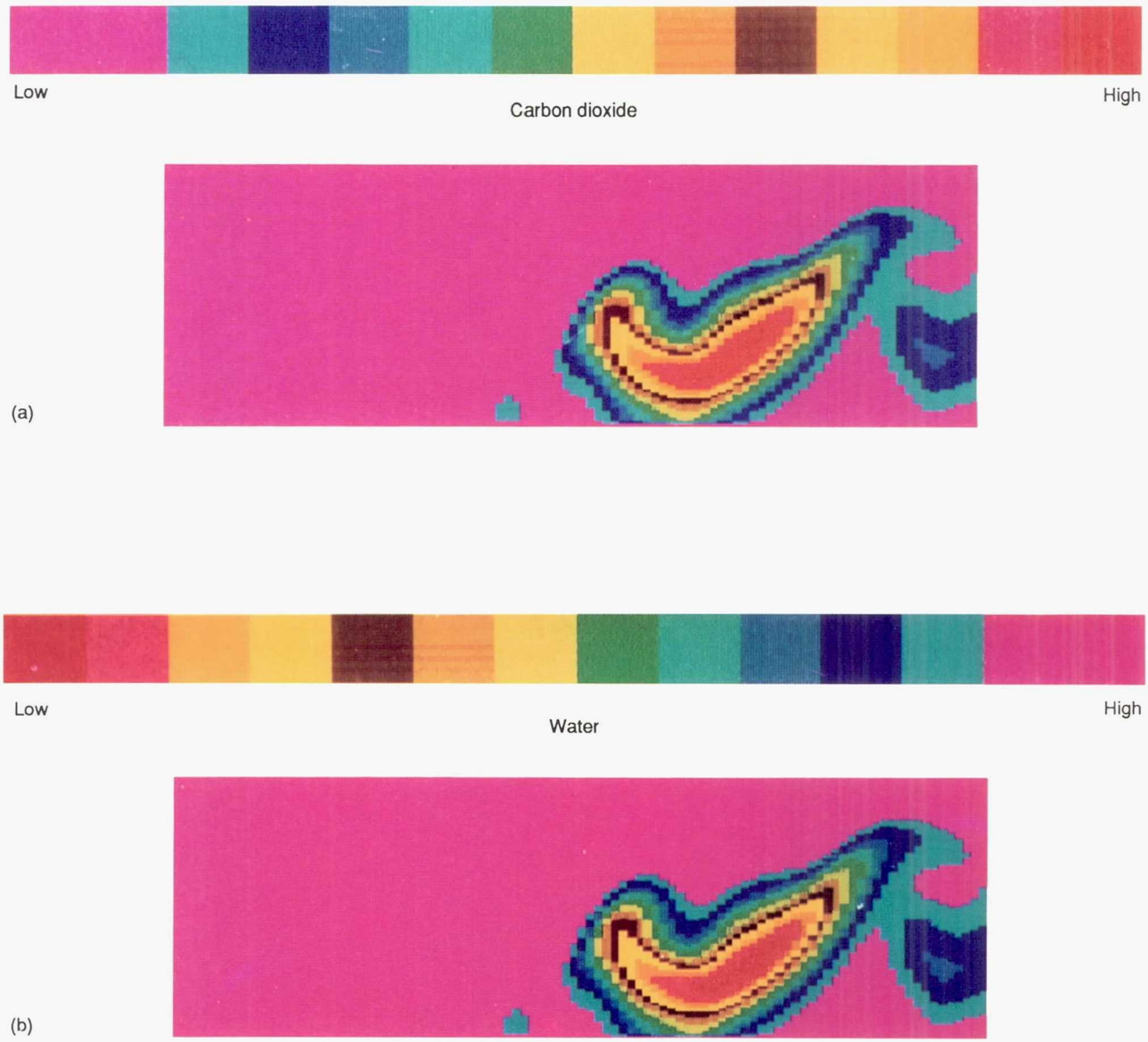

(a) Carbon dioxide distribution.
(b) Water distribution.

Figure 8.—Carbon dioxide and water distributions along the combustor for a rich-zone equivalence ratio of 1.40.

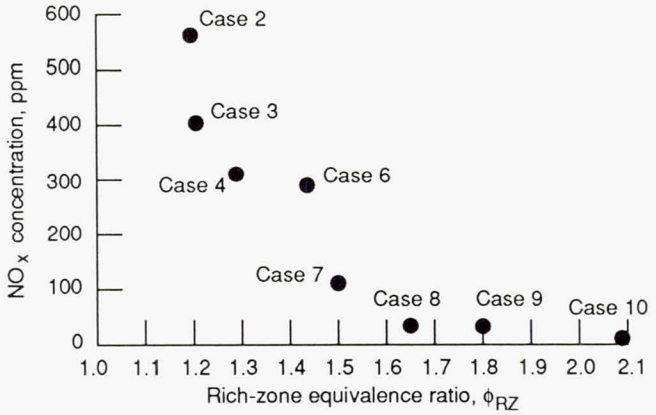

Figure 9.—NO_x concentration as a function of rich-zone equivalence ratio for RQL combustor.

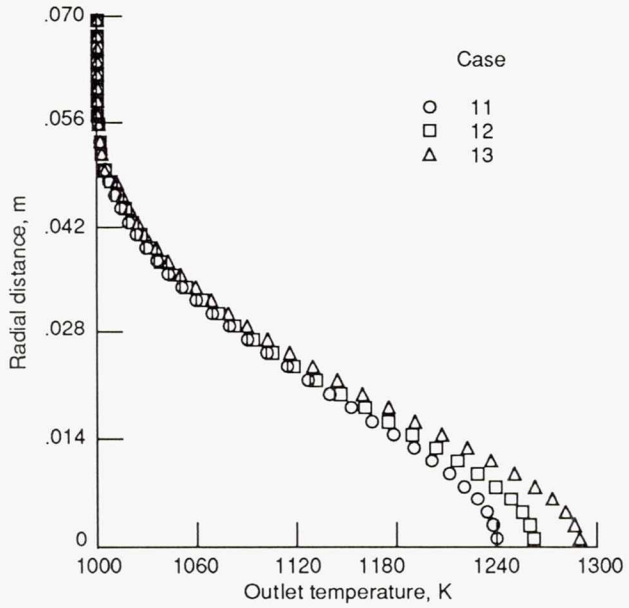

Figure 10.—Typical outlet temperature profiles for RQL combustor.

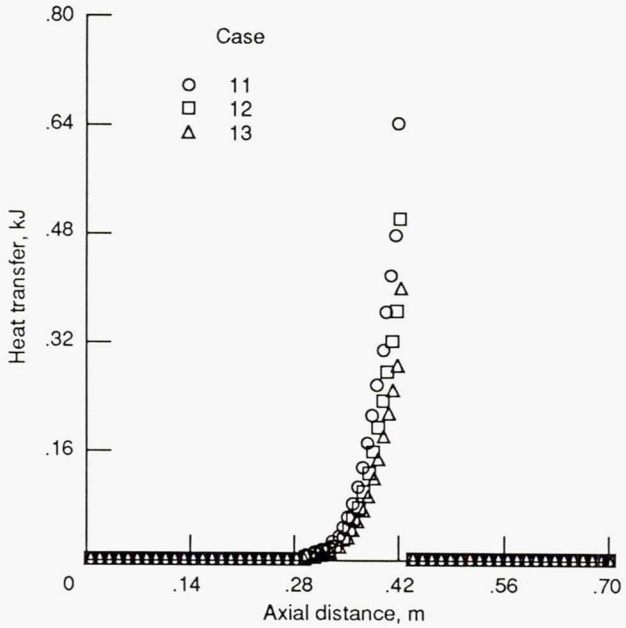

Figure 11.—Typical local liner heat transfer profiles for RQL combustors.

Concluding Remarks

A mathematical model and a computer program were developed to study the flow field, combustion, and exhaust gas emissions of a low NO_x, staged combustor representative of the Rich Burn/Quick-Quench Mix/Lean Burn concept. The two-dimensional axisymmetric combustor consisted of a primary and a secondary zone.

The model solved the two-dimensional equations of continuity, momentum, energy, and chemical species as well as a two-equation model of turbulence. Discrete equations were solved by the semi-implicit method for pressure-linked equations (SIMPLE). Turbulent boundary layers were resolved with law-of-the-wall equations, and wall heat fluxes were calculated from the Reynolds analogy between momentum and heat transfer. The oxidation of the fuel was modeled by using a quasi-global kinetic mechanism, and this reaction rate was modeled by a mixing-controlled model. The amount of nitric oxide formation was computed for a variety of operating conditions by using the Zeldovich mechanism.

The calculations indicate that high turbulence and mixing yield high reaction rates and high flame temperatures in addition to good combustion efficiency. The predicted NO_x formation is a function of flame temperature, residence time, and oxygen availability. Our findings, however, show that quick-quench mixing and dilution jets in gas turbine combustors constitute a fully three-dimensional problem that must be simulated by using a three-dimensional cylindrical coordinate system. The two-dimensional simulation of the quick-quench mixing and dilution jets in this study results in local quenching of the reaction in the quick-quench region, which is due to the high flow rate of air injected through the two-dimensional hole on the combustor liner. Future work will focus on developing a three-dimensional version of the present technique and extending the mixing-controlled model to include more chemical species and chemical reactions.

References

1. Pierce, R.M.; Smith, C.E.; and Hinton, B.S.: Low NO_x Combustor Development for Stationary Gas Turbine Engines, Proceedings of the Third Stationary Source Combustion Symposium, EPA-600/7-79-050C, Vol. III, Feb. 1979.
2. Kemp, F.S.; Sederquist, R.A.; and Rosfjord, T.J.: Evaluation of Synthetic-Fuel Character Effects on Rich-Lean Stationary Gas Turbine Combustion Systems, United Technologies Corp., South Windsor, CT, EPRI AP-2822, Vols. I and II, Final Report, Feb. 1983.
3. Lew, H.G.; et al.: Low NO_x Heavy Fuel Combustor Concept Program, Phase I: Combustion Technology Generation, NASA CR-165482, 1981.
4. Nowick, A.S.; and Troth, D.L.: Low NO_x Heavy Fuel Combustion Concept Program, NASA CR-165367, 1981.
5. Nguyen, H.L.; Bittker, D.A.; and Niedzwiecki, R.W.: Investigation of Low NO_x Staged Combustor Concept in High-Speed Civil Transport Engines, AIAA Paper 89-2942, July 1989 (also NASA TM-101977, 1989).
6. Gleason, C.C.; and Bahr, D.W.: The Experimental Clean Combustor Program, (ECCP), Phase III—Commercial Aircraft Turbofan Engine Tests with Double Annular Combustor: Final Report, NASA CR-135384, 1978.
7. Rudey, R.A.; and Reck, G.M.: Advanced Combustion Techniques for Controlling NO_x Emissions of High Altitude Cruise Aircraft, NASA TM X-73473, 1976.
8. Roeffe, G.: Effect of Inlet Temperature and Pressure on Emissions from a Premixing Gas Turbine Primary Zone Combustor, NASA CR-2740, 1976.
9. Ramos, J.I.: Numerical Solution of Non-Premixed Reactive Flows in a Swirl Combustor Model, Engineering Computations, Vol. 1, 1984, pp. 173-182.
10. Hinze, J.O.: Turbulence, 2nd ed., McGraw-Hill, New York, 1975.
11. Ramos, J.I.: Incompressible Swirling Flows, Engineering Computations, Vol. 3, 1986, pp. 51-63.
12. Patankar, S.V.: Numerical Heat Transfer and Fluid Flow, Hemisphere, New York, 1980.

NASA
National Aeronautics and Space Administration

Report Documentation Page

1. Report No.	2. Government Accession No.	3. Recipient's Catalog No.
NASA TM-103236		

4. Title and Subtitle	5. Report Date
Application of Mixing-Controlled Combustion Models to Gas Turbine Combustors	6. Performing Organization Code

7. Author(s)	8. Performing Organization Report No.
Hung Lee Nguyen	E-5649
	10. Work Unit No. 537-02-11

9. Performing Organization Name and Address	11. Contract or Grant No.
National Aeronautics and Space Administration Lewis Research Center Cleveland, Ohio 44135-3191	13. Type of Report and Period Covered Technical Memorandum

12. Sponsoring Agency Name and Address	14. Sponsoring Agency Code
National Aeronautics and Space Administration Washington, D.C. 20546-0001	

15. Supplementary Notes

Prepared for the Joint Symposium on General Aviation Systems, cosponsored by the AIAA and FAA, Ocean City, New Jersey, April 11-12, 1990.

16. Abstract

This report describes the study of exhaust gas emissions from a staged Rich Burn/Quick-Quench Mix/Lean Burn (RQL) combustor under test conditions encountered in High Speed Research (HSR) engines. The combustor was modeled at conditions corresponding to different engine power settings, and the effect of primary dilution airflow split on emissions, flow field, flame size and shape, and combustion intensity, as well as mixing, was investigated. A mathematical model was developed from a two-equation model of turbulence, a quasi-global kinetics mechanism for the oxidation of propane, and the Zeldovich mechanism for nitric oxide formation. A mixing-controlled combustion model was used to account for turbulent mixing effects on the chemical reaction rate. This model assumes that the chemical reaction rate is much faster than the turbulent mixing rate. The work described in this report is a part of the NASA High Speed Research Low NO_x program.

17. Key Words (Suggested by Author(s))	18. Distribution Statement
Mixing-controlled combustion models Premixed and diffusion flames Rich Burn/Quick Mix/Lean Burn combustors	Unclassified – Unlimited Subject Category 07

19. Security Classif. (of this report)	20. Security Classif. (of this page)	21. No. of pages	22. Price*
Unclassified	Unclassified	14	A03

*For sale by the National Technical Information Service, Springfield, Virginia 22161